JOURNAL OF NUCLEAR MEDICINE 7:32-40, 1966

Correlation of Brain Scan Image and Area Counting After Scanning With Tumor Pathology[2,3]

Mutsumasa Takahashi, M.D., Mohammed M. Nofal, M.D. and William H. Beierwaltes, M.D.[1]

Ann Arbor, Michigan

Multiple point counting (1) and mechanical scintillation scanning (2) have each been used with some success in the diagnosis of brain tumors, as verified by findings at surgery or autopsy. Area counting after scanning has proved helpful to use in roughly quantifying the per cent uptake of ^{131}I in thyroid carcinoma metastases relative to non-involved tissue in a comparable area of anatomy (3). We have, therefore, attempted to evaluate the aid that area counting after brain tumor scanning might offer. We have determined the relative per cent uptake of ^{197}Hg or ^{203}Hg Neohydrin in brain tumor tissue as compared to non-involved brain tissue in 102 histologically verified cases with positive brain scans. Pathological diagnoses of the tumors have been correlated with this data as well as with the location, size and configuration of the positive scan image of the brain tumor, in an attempt to correlate histological and scintiscan findings.

METHODS

Photoscanner

Scintiscans were made with a photo-dot recording system equipped with a three by two inch NaI crystal, a pulse height analyzer, and a 19 hole collimator[4]. The pulse height analyzer was set to accept peak energies for ^{203}Hg and ^{197}Hg.

---

[1]Departments of Radiology and Medicine (Nuclear Medicine), University of Michigan Medical School, Ann Arbor, Michigan.

[2]This work was supported in part by the Nuclear Medicine Research Fund.

[3]Presented to the Twelfth Annual Meeting of the Society of Nuclear Medicine, Bal Harbour, Florida, June 1965.

[4]Picker Magnascanner, Picker X-ray Corporation, White Plains, New York.

Scan and Area Counting Technique

Scans were performed with ^{203}Hg chlormerodrin or ^{197}Hg chlormerodrin, the former primarily used before January, 1963. The radioactive material was injected intravenously in a dose of 10μC/kgm body weight (^{203}Hg) or 15μC/kg body weight (^{197}Hg), three to six hours before scanning. Except for emergency brain scans, 1 ml of stable chlormerodrin was given intramuscularly 24 hours prior to the scan in an attempt to reduce the accumulation of radiomercury in the kidneys. Routinely, two views were obtained depending upon the site of the lesion as suspected clinically. After the scan was completed, count rates (c/m) were recorded over areas of apparently normal brain and over the areas demonstrating above normal concentrations of radioactivity. The motion of the scanner was stopped for these counts with the collimator centered over the center of the above normal area of concentration of the radioisotope. These counts were expressed as a differential uptake ratio, as obtained from the lateral scan.

The differential uptake ratio was defined as the ratio of the area counting (c/m) over the localized concentration of radioactivity to the background over adjacent normal brain tissue. No correction was made for size or location of tumors.

Configuration of Scan Image

Brain tumor scan images were classified as;

a) spherical outline with sharp margin
b) spherical outline with irregular margin, and
c) non-spherical outline with irregular margin (Table II).

Scans were not included when it was apparent that the patient moved during the scanning procedure, or concentration was not sufficient to outline the lesion.

Location of Tumors

Brain tumors were classified by anatomical location. No lesion was included under more than one heading, and the most extensively involved area was chosen when more than one area was involved by a lesion.

Size of Tumors

Measurements of the positive scan image were made with a centimeter ruler. When the lesion was non-spherical, two or three measurements were taken and averaged.

Case Material

One hundred and two histologically verified cases with positive brain scans were reviewed. Scans were all performed in the Clinical Nuclear Medicine Unit of the University of Michigan Medical Center from January 1962, to October 1964. Of the 102 patients, 21 had meningiomas, 16 had astrocytomas, 28 had glioblastoma multiforme and 23 had metastatic carcinomas. Of the remaining 14

patients, there were three brain abscesses, two ependymomas, two acoustic neurinomas, and single cases of neuroastrocytoma atrionare, oligodendroglioma, A-V malformation, primary lymphoblastoma, craniopharyngioma, chemodectoma and pituitary adenoma. The classification of gliomas by Kernohan and Sayre (4) was used in this study. "Astrocytoma" indicated astrocytoma grade I and II, whereas, designation of glioblastoma multiforme was used for astrocytoma grade III and IV.

RESULTS

Differential Uptake Ratio

The differential uptake ratio was available in 60 out of 102 scans (Table I). The glioblastomas and meningiomas showed the highest average ratios, followed by metastatic carcinomas and astrocytomas. The latter two showed similar ratios. The number of other entities was too small to permit a definite conclusion.

Although there was considerable overlap between groups in differential uptake ratios in individuals, there was a significant difference ($<0.05 > 0.01$) in differential uptake ratio between the groups as follows; glioblastomas > meningiomas > astrocytomas and metastatic carcinomas.

Configuration of Brain Scan Image

It was possible to classify 95 intracranial tumors by the configuration of the brain scan image (Table II).

Of the 28 glioblastomas, nine had non-spherical concentration of radioisotope with irregular outlines, whereas, 10 of the 21 meningiomas produced spherical, sharply marginated images. The remaining tumors in these two groups were usually spherical with irregular margins. Astrocytomas and metastatic carcinomas also had a tendency to be spherical in shape with an irregular margin, as did the other pathologic entities.

TABLE I. DIFFERENTIAL UPTAKE RATIO

Diagnosis	*No. of Patients*	*Average Ratio*
Meningioma	14	2.7
Astrocytoma[1])	12	2.3
Glioblastoma multiforme[2])	16	3.1
Metastatic carcinoma	12	2.4
Abscess	3	2.2
Pituitary adenoma	1	1.5
Acoustic neurinoma	1	2.6
Primary lymphoblastoma	1	2.6

[1])Astrocytoma grade I and II
[2])Astrocytoma grade III and IV

Location and Histologic Types of Tumors

Locations of 99 intracranial lesions were classified as in Table III.

Of the 21 meningiomas in this series, seven were localized in the parasagittal area, four in the anterior fossa, and three in the parasylvian region or parietal area. Four anterior fossa lesions included three sphenoid ridge and one olfactory groove meningiomas. Gliomas and metastatic carcinomas were rarely found in this area.

Twenty-seven of 28 glioblastomas and six of 16 astrocytomas were distributed equally in each part of the cerebrum. Ten astrocytomas were in the posterior fossa and six glioblastomas were in the paraventricular region. No meningiomas were detected in the paraventricular region.

Metastatic carcinomas in 23 patients were encountered widely in the cerebrum and cerebellum with a relatively high incidence in the occipital (10 of 27 lesions) and parietal (5 of 27 lesions) regions. There were four patients who showed more than one lesion on the same scan and all proved to harbor metastatic carcinoma. Primary lesions were found in the lung in eight of the 23 patients, in the breast of four, and in the colon or uterus in three patients.

Of the 18 posterior fossa tumors, there were 10 astrocytomas, three metastatic carcinomas, three ependymomas, two acoustic neurinomas and single instances of neuroastrocytoma and meningioma. No pontine glioma was detected.

Size of Tumors

The average diameter of 99 intracranial lesions is tabulated in Table IV.

Although there was considerable overlap in tumor size between groups in individuals, there was a significant difference ($<0.05 > 0.01$) in size between the tumor groups as follows; glioblastomas and meningiomas > astrocytomas and metastatic carcinomas.

TABLE II. CONFIGURATION OF TUMORS

Diagnosis	*No. of Patients*	*Spherical; Sharp Margin*	*Spherical; Irregular Margin*	*Non-spherical; Irregular Margin*
Meningioma	21	10	10	1
Astrocytoma	16	4	12	0
Glioblastoma multiforme	28	4	15	9
Metastatic carcinoma	23	4	17	2
Abscess	3	1	1	1
Ependymoma	2	0	2	0
Acoustic neurinoma	2	0	2	0
Total	95	23	59	13

TABLE III. LOCATION OF TUMORS

Diagnosis	*No. of Lesions*	*Frontal*	*Parietal*	*Temporal*	*Occipital*	*Parasylvian*	*Parasagittal*	*Paraventricular*	*Anterior Fossa*	*Middle Fossa*	*Posterior Fossa*
Meningioma	21	1	3	0	2	3	7	0	4	0	1
Astrocytoma	16	1	1	1	0	1	1	1	0	0	10
Glioblastoma multiforme	28	5	5	7	2	0	2	6	1	0	0
Metastatic carcinoma	27	1	5	2	10	1	2	0	1	2	3
Abscess	3	0	3	0	0	0	0	0	0	0	0
Ependymoma	2	0	0	0	0	0	0	0	0	0	2
Acoustic neurinoma	2	0	0	0	0	0	0	0	0	0	2
Total	99	8	17	10	14	5	12	7	6	2	18

DISCUSSION

Differential Uptake Ratios

Sweet and his associates (5) reported differential uptake ratios in various types of intracranial neoplasms on biopsied specimens after injection of positron emitting arsenic and copper. They demonstrated that meningiomas showed the highest value, followed in order of decreasing concentrations by acoustic neurinomas, glioblastomas, metastatic carcinomas and astrocytomas. Brinkman, Wegst, and Kahn, in our laboratory (6), and McAfee and Taxdal (7) believed from the

TABLE IV. SIZE OF TUMORS

Diagnosis	*No. of Lesions*	*Average Diameter (cms)*
Meningioma	21	4.4
Astrocytoma	16	3.6
Glioblastoma multiforme	28	4.7
Metastatic carcinoma	27	3.8
Abscess	3	4.7
Ependymoma	2	2.5
Acoustic neurinoma	2	4.0

apparent density of the visual image that meningiomas and glioblastomas showed the highest concentrations of ^{203}Hg Neohydrin. Feindel and co-workers (8) came to a similar conclusion using contour brain scanning with iodide and Hg compounds. Our results on patients with radioactive Hg scans followed by area counting are in keeping with these reports except that glioblastomas concentrated radio-mercury more avidly than meningiomas.

Brinkman and co-workers (6) also suggested that glioblastomas and meningiomas were detected more successfully than metastatic carcinomas and astrocytomas. Our results using the differential uptake ratio after scanning corresponds with this stated ease of detecting various intracranial tumors.

We have no evidence to date that area counting alone makes a diagnosis possible when the scan is negative. It is an additional bit of data, however, that reinforces the impression in instances where the image is doubtful.

In our hands area counting has been easier and more reliable than counting the relative number of dots per unit area on the scan.

Configuration

The glioblastoma (Fig. 1) tends to infiltrate adjacent brain tissue, frequently forming butterfly-type or multiform tumors (4, 9). In our study, approximately 30 per cent of glioblastomas exhibited these patterns.

The meningioma has been described by others as a round, sharply circumscribed mass without infiltration. Our data indicated that roughly one-half of meningiomas presented as spherical, sharply outlined images (Fig. 2).

The images produced by metastatic carcinomas and astrocytomas also were generally fairly well circumscribed in this series. When metastatic lesions appeared as multiform or dumb bell type images, they were frequently difficult to differentiate from glioblastomas. The presence of two or more separate lesions, however, strongly suggests the diagnosis of metastatic carcinoma (Fig. 3) since other pathologic entities rarely presented as multiple lesions.

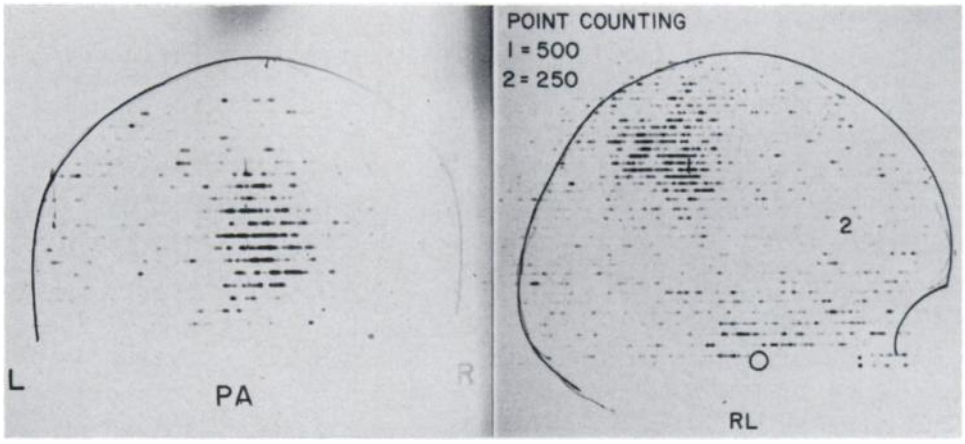

Fig. 1. Posteroanterior and right lateral ^{203}Hg scan demonstrating a 4 x 4 x 4 cm multiform lesion in the right posterior parietal region. This was a glioblastoma with differential uptake ratio of 2.0.

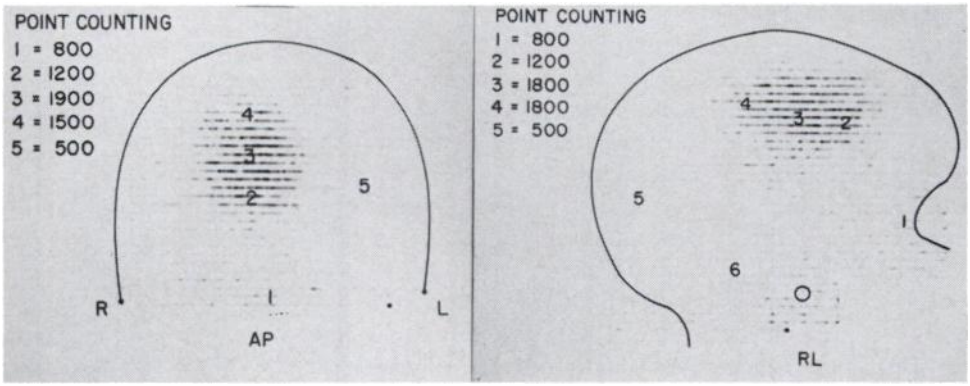

Fig. 2. Anteroposterior and right lateral ^{197}Hg scan showing a 6 x 6 x 6 cm. well marginated recurrent meningioma in the parietal parasagittal region. Differential uptake ratio was 3.6.

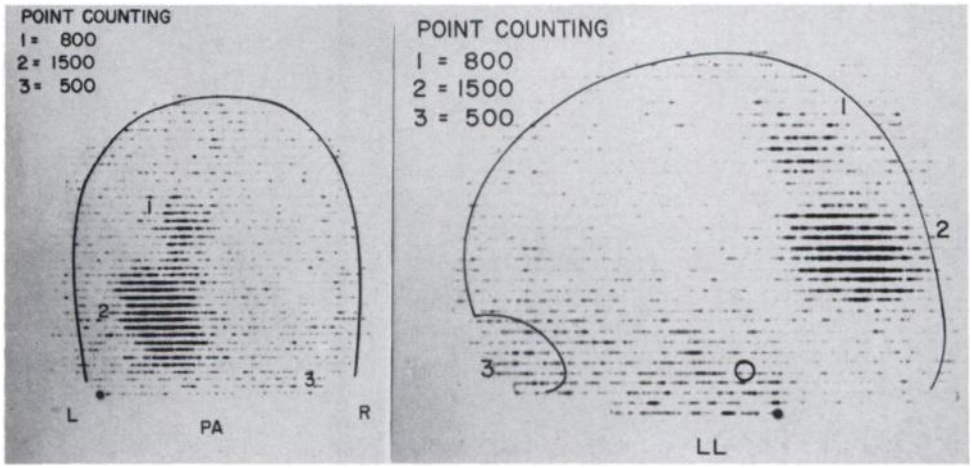

Fig. 3. Posteroanterior and left lateral ^{203}Hg brain scan showing a 6 x 5 x 5 occipital lesion and a 3 x 3 x 3 cm posterior parietal lesion. Differential uptake ratios were 3.0 and 1.6, respectively. These sharply marginated lesions were proved to be metastatic carcinoma.

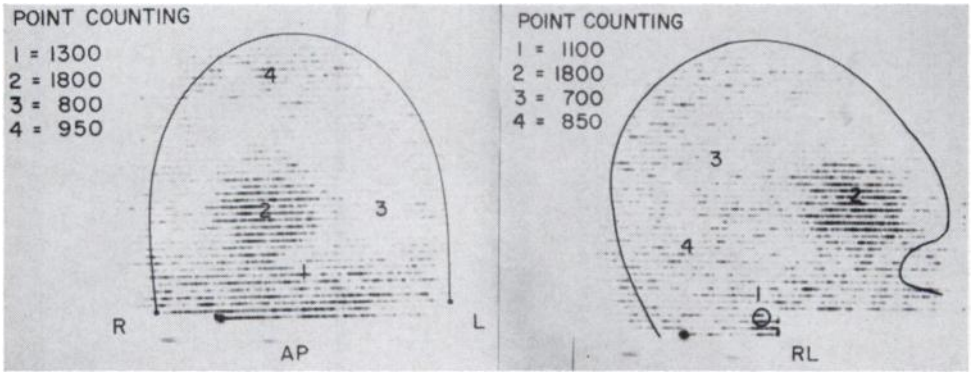

Fig. 4. Anteroposterior and right lateral ^{197}Hg brain scan with a sharply marginated abnormal concentration in the right frontal region. This was an astrocytoma with differential uptake ratio of 2.3.

Location

More than 56 percent of meningiomas were localized in parasagittal areas, sphenoid ridges, olfactory grooves and parasylvian areas, but meningiomas in the convexities of cerebral hemispheres were relatively uncommon. As might be expected, astrocytomas (Fig. 4) and glioblastomas occurred in each portion of the brain with fairly equal frequency, with the exception of a high incidence of astrocytomas in the posterior fossa (Fig. 5).

It is noteworthy that most of the deep-seated or paraventricular tumors proved to be glioblastomas or astrocytomas. Metastatic lesions were most frequently found in the occipital, posterior temporal and posterior parietal areas. This observation is supported by Kindt (10) who reported that a definite site of predilection for metastatic tumors is found near the junction of the temporal, parietal and occipital lobes. Meningiomas were rarely found in this location. Our scans were less accurate for detection of lesions in the brain stem, pituitary fossa and deep-seated areas as reported by other investigators (2, 8). Posterior fossa tumors have also been considered less amenable to localization by brain scanning (2). Our ability to detect posterior fossa tumors by scanning was fairly good in spite of large venous sinuses, upper cervical muscles, and mastoids which produce high background on scans. In another study (11), 29 of 41 cases or 71 percent of all posterior fossa tumors were localized accurately. Cerebellar astrocytomas, metastatic carcinomas, ependymomas and acoustic neurinomas were the common lesions detected by the brain scan in this area.

Size

It is commonly agreed that meningiomas grow slowly and frequently do not produce symptoms until they become relatively large, while glioblastomas increase in size very rapidly. Both of these intracranial tumors were found to be large in size in this series. On the contrary, astrocytomas and metastatic carcinomas were relatively smaller.

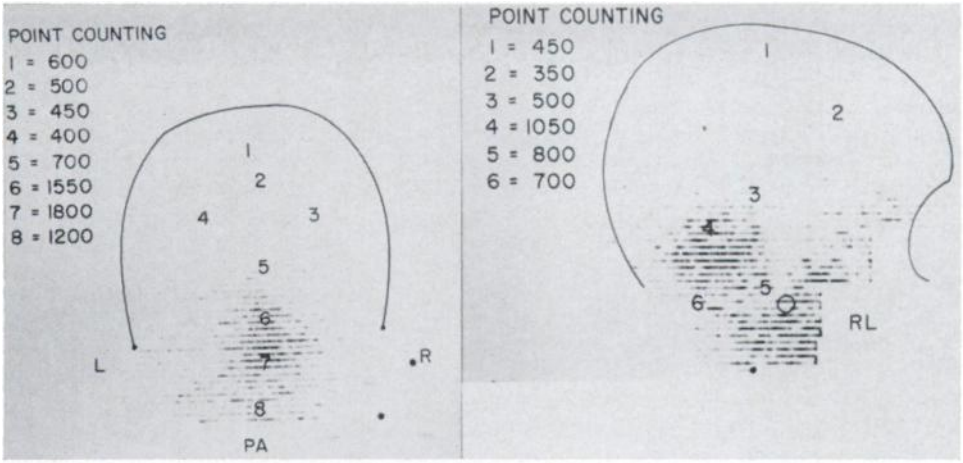

Fig. 5. Posteroanterior and right lateral ^{197}Hg scan showing a 4 x 3 x 3 cm midline cerebellar astrocytoma with sharp margin. Differential uptake ratio was 3.0.

SUMMARY AND CONCLUSION

One hundred and two brain scans with histologically verified brain tumors were studied in an attempt to correlate brain scans and area counting findings with tumor pathology. The following trends were noted;

1. Meningiomas commonly show sharply demarcated, round concentrations with moderately high differential uptake ratios. They are frequently large and localized in the parasagittal, parasylvian, sphenoid ridge and olfactory groove regions.
2. Astrocytomas usually present as small, round concentrations with frequent localization in the posterior fossa and low differential uptake ratios. The distribution in the cerebrum is usually wide.
3. Glioblastomas are frequently present as large, irregular isotope concentrations with high differential uptake ratios. Most deepseated tumors seen on brain scans are glioblastomas.
4. Metastatic carcinomas appear to be small and round with low differential uptake ratios. They are frequently found in occipital, posterior parietal, and posterior temporal regions. They are the most common cause of more than one positive image on a brain scan.
5. The most common types of posterior fossa tumors seen on brain scans are cerebellar astrocytomas, metastatic carcinomas, acoustic neurinomas and ependymomas. Accuracy of detecting these tumors by scans is approximately 70 percent.

REFERENCES

1. PLANIOL, T.: Diagnostic des lesions intracraniennes par la gamma—encephalographie a l'aide de la serum albumine humaine marquee a l'iode 131. *Medical Radioisotope Scanning, Vienna. International Atomic Energy Agency*, p. 189, 1959.

2. MCAFEE, J. G., AND FUEGER, G. F.: The value and limitations of scintillation scanning in the diagnosis of intracranial tumors. *Scintillation Scanning in Clinical Medicine*, edited by J. L. Quinn, III, Philadelphia: W. B. Saunders Co., p. 183, 1964.

3. HAYNIE, T. P., NOFAL, M. M., AND BEIERWALTES, W. H.: Treatment of thyroid carcinoma with I-131: Results at fourteen years. *J.A.M.A.* **183**:303, February 2, 1963.

4. KERNOHAN, J. W., AND SAYRE, G. P.: Tumors of the central nervous system. *Atlas of Tumor Pathology by the Armed Forces Institute of Pathology, Washington, D.C.*, Armed Forces Institute of Pathology, Section X, Fascicles 35 and 37, pp. 22, 97, 1952.

5. SWEET, W. H., MEALEY, J., JR., BROWNELL, G. L., AND ARONOW, S.: Coincidence scanning with positron-emitting arsenic or copper in the diagnosis of focal intracranial disease. *Medical Radioisotope Scanning, Vienna. International Atomic Energy Agency*, p. 163, 1959.

6. BRINKMAN, C. A., WEGST, A. V., AND KAHN, E. A.: Brain scanning with mercury-203 labeled Neohydrin. *J. Neurosurg.* **19**:644, August 1962.

7. MCAFEE, J. G., AND TAXDAL, D. R.: Comparison of radioisotope scanning with cerebral angiography and air studies in brain tumor localization. *Radiology* **77**:207, August 1961.

8. FEINDEL, W., YAMAMOTO, Y. L., MCRAE, D. L., AND ZANELLI, J.: Contour brain scanning with iodine and mercury compounds for detection of intracranial tumors. *Am. J. Roentgenol.* **92**:177, July 1964.

9. RUSSELL, D. S., AND RUBINSTEIN, L. J.: Pathology of tumours of the nervous system. London: Edward Arnold (Publishers) Ltd., pp. 43, 143, 1959.

10. KINDT, G. W.: The pattern of location of cerebral metastatic tumors. *J. Neurosurg.* **21**:54, January 1964.

11. TAKAHASHI, M., AND BEIERWALTES, W. H.: Unpublished data.